Voltage Source Converter Control Under Unbalanced Grid Voltage

Ahmed G. Abo-Khalil and Ali M. Eltamaly

Abstract The conventional control of the voltage source converter (VSC) assumes that the input voltage is balanced. However, unbalanced voltage is a phenomenon that occurs frequently in actual industrial sites. If the grid voltage is unbalanced, THD increases due to voltage negative component, and low harmonic components appear in DC-link voltage, which adversely affects the performance of the converter. Therefore, the purpose of this study is to propose an efficient control method that can solve the problem of the AC-DC converter due to the unbalance of grid voltage. A Multivariable State-Feedback (MSF) current controller is proposed to improve the performance of the VSC under grid voltage disturbances. The control process is carried out by adjusting the extracted positive and negative components of the grid d and q-axis currents. To minimize the DC-link voltage ripple, the reference negative grid currents are obtained from the DC-link voltage controller. However, if the target is to eliminate the imbalance of the grid current, the reference negative currents are set to zero. The experimental results are discussed to validate the proposed controller. The results show that the new MSF controller reduced the DC-link ripple and provides a fast dynamic response during unbalanced grid voltage.

Keywords Voltage source converter · Unbalanced grid voltage · MSF · PI controller

A. G. Abo-Khalil
Assiut University, Assiut, Egypt

School of Electrical and Computer Engineering, Yeungnam University, Gyeongsan, South Korea

A. M. Eltamaly (✉)
Mansoura University, Mansoura, Egypt
e-mail: a.abokhalil@mu.edu.sa; eltamaly@ksu.edu.sa

King Saud University, Riyadh, Saudi Arabia

A. M. Eltamaly et al. (eds.), *Control and Operation of Grid-Connected Wind Energy Systems*, Green Energy and Technology,
https://doi.org/10.1007/978-3-030-64336-2_3

1 Introduction

The current electrical systems are dominated by large generating plants that are located at a great distance from the consumption centers and near the primary energy sources. This centralized model requires the construction of transmission lines to transport electrical energy and is characterized by having an acceptable cost–benefit ratio. However, the growing motivation to exploit resources locally, the tendency to stop relying on a single source of generation, and the need to reduce the emission of greenhouse gases (e.g., CO_2) into the atmosphere, creates the need to explore new alternatives to the centralized model [1].

Distributed generation (DG) emerges as a new option to the centralized model. This consists of the use of electric energy sources with powers and voltages below 10 MVA and 69 kV respectively, in order to generate energy locally and near the consumption centers. Generation from batteries, micro-turbines, solar panels, wind turbines, etc., are some of the clearest examples of this type of generation [2].

Loads using semiconductor power converters such as motor drive systems computer systems, etc., operate as nonlinear loads and are the main cause of generating serious harmonics on the power side. Such harmonic current can distort the power supply voltage and insulation breakdown or shortening of the lifespan of various power facilities such as electric devices, cables, and high-phase capacitors. Moreover, due to the nonlinear load, harmonic currents flow into the Point of Common Coupling (PCC) which makes the voltage distorted at the PCC and may cause the thermal overload of the power transformer. In addition, it causes malfunction or EMI phenomenon of various electronic equipment such as measuring equipment and causes electronic environmental problems such as interference in the communication system. In addition, abnormal vibration torque is generated in the motor, and losses such as iron loss and copper loss are increased [3, 4]. Recently, several types of active power filters are proposed [5] to minimize the harmonic distortion in the grid side and to compensate for the source voltage unbalance and sag. However, it is not an economical and effective method since the active power filter cannot be installed for every nonlinear load.

Advances in DG allow the use of new technologies that make the exploitation of electricity networks more flexible and secure. The integration of DG in electrical systems allows: Increase the degree of stability of the network, increase the levels of penetration of renewable energies, increase the limits of stability of the electrical system and improve the quality of energy [3].

Ideally, the voltages in the electrical systems are balanced, however, due to the existence of nonlinear and unbalanced loads, differences in the voltage levels of each of the phases of the network are presented.

Among the devices used to mitigate this type of disturbances is the voltage-controlled converter or (Voltage Source Converters) VSC whose connection is in parallel and its operation consists in general terms in the injection of compensation currents to mitigate disturbances related mainly to the currents demanded

by disturbing loads. Articles in the technical literature and reporting control structures for power converters normally use PI controllers [6, 7]. These PI controllers require extensive knowledge of the system and must linearize and work at a point of operation. In fact, the converters are non-linear systems and, due to the change in the operating point, they may work improperly. The implementation of the control for electronic-based converters normally requires cascade controls with an internal current PI control loop and an external voltage PI control loop, this requires that the PI controllers be very well-tuned and that a relatively large capacitor is necessary to minimize the DC-link voltage ripple. To overcome this issue, nonlinear controllers such as back-stepping control [8], passivity-based control [9–11], and slid-mode control [12], direct power control [13] have been proposed by several researchers. Also, the input–output linearization based on feedback linearization has been applied for VSC control [14]. The main reason to use this control method is the ability to transform the nonlinear system into an uncoupled linear system. Then, a linear controller can be used to ensure stability throughout the entire operating range of the converter. It is interesting to note that when the DC voltage is selected as an output to be controlled in the exact linearization, the VSC is not completely linearizable and then a nonlinear internal dynamics appears that is unstable [15]. To overcome this inconvenience, internal current control loops are generally considered, where the exact linearization can be applied considering the currents as output. Then, a slower external DC voltage control loop is designed via a cascading PI control [16–18].

However, in actual three-phase power systems, the supply voltage is often distorted or unbalanced due to nonlinear loads and imbalance of steady-state loads which are connected to the point of common coupling (PCC). During unbalanced grid voltage operation, a negative component for grid voltage and current exists and produces oscillations of both active and reactive powers at the double- frequency of the grid. In this case, a dual current controller is proposed to separate the grid current into normal and reverse phases to eliminate the ripple of DC-link voltage [19, 20]. A method of using a proportional resonant current controller has been proposed to eliminate the effect of the unbalanced grid voltage in [21, 22]. However, using a dual current controller adds more complications for the controller design and gain calculations. Besides, this controller can compensate for the harmonic distortions in the resonance frequency only without compensating the other components. A method of predicting the future current and power components is introduced based on the predictive control method [23, 24].

2 The Requirement for Generation Interconnection Distributed to the Grid

The connection of DG to the power grid must meet a series of technical requirements to achieve efficient and safe operation in the presence of these. In particular, the voltages and currents in the network must be maintained at all times in their admissible

ranges and the quality of service and power of the clients connected to the network in the area of influence of the generator must not be degraded. This translates on the one hand into operating conditions and restrictions that are imposed on the distributed generator to authorize it to inject power into the network, and on the other hand, the connection of the generator to the network is to assess the feasibility of certain proposed connectivity. Both concepts are denoted in the so-called "connection criteria" for distributed generation. These DG connection criteria are established based on the current electrical regulations applicable to the network planning and operation distribution system, and international standards of reference in the field. Among the latter, the "1547 IEEE Standard for Interconnecting Distributed Resources with Electric Power Systems" standard stands out.

The IEEE 1547 standard provides a set of requirements for the interconnection of distributed resources with EPS (electrical energy systems) for performance, operation, testing, safety, and maintenance of the interconnection.

Justification is made from the perspective of the distributor of some of the distributed generation connection criteria established in the IEEE 1547 standard, and their formulation and practical implementation are described and exemplified, among the most important connection criteria are:

A. Voltage Regulation at the Connection Point
   The distributed generator is required not to actively regulate the voltage at the connection node. It is then considered that at the distribution level the generator connection node is a PQ (load) node and not a PV (generation) node as usual in generators connected to the transmission network. One of the justifications for this criterion is to minimize the chances that the distributed generator will be operating on an unintentional island. Another argument that supports the criterion is that there is no interference with the mechanisms and equipment of voltage regulation, for example, the case of current-controlled line voltage regulators. It is admitted that the distribution unit may require the generator to maintain the power factor measured at the point of coupling with the network within a given range (0.95–1.05), to help maintain the voltage profiles of the network within acceptable values by $\pm$ 5% without causing fluctuations.
B. Tensions in the Network under Normal Operating Regime
   The criterion establishes that the presence of DG should not cause the voltage in the network nodes to exceed the regulatory limits for any state of network load and power injected by the generator. This criterion applies to the design of the connection of the generator to the electricity grid and for the operation of the network once the generator is connected, this makes the most restrictive case for the design and operation of the scenario of minimum load in the network, with the generator injecting all its authorized active power. Under these conditions, it must be ensured that the voltages in the network do not exceed the maximum permissible value, in the normal operating configuration. The range of admissible voltages varies according to the voltage level. A typical value is 5% around the nominal voltage value.

3 VSC Model During Unbalanced Grid Voltage

The voltage-controlled converters or VSC are one of the most used topologies in DG systems and high voltage transmission systems in direct current, with controlled magnitude and phase. This is achieved through the correct switching of the IGBTs, which are characterized by being efficient at the high switching frequency, reliable, and easily acquired in the market. Many of the control strategies used for these converters need to detect the fundamental component of the positive sequence of the network to determine the reference signals necessary to carry out the control.

These positive sequence detection methods are necessary to achieve the correct compensation between the GD-based generation systems and the power grid that are connected.

The apparent power of the VSC, in Fig. 1, during the grid unbalanced voltage can be written in terms of the positive and negative components of the grid voltage and current as [25]

$$S = P + jQ = E_{\alpha\beta} \cdot \bar{I}_{\alpha\beta} = \frac{\left[e^{(j\omega t)}\left(E_d^p + jE_q^p\right) + e^{(-j\omega t)}\left(E_d^n + jE_q^n\right)\right]}{\left[e^{(j\omega t)}\left(I_d^p + jI_q^p\right) + e^{(-j\omega t)}\left(I_d^n + jI_q^n\right)\right]} \quad (1)$$

where "p" and "n" are the subscripts of the positive and negative components, respectively. The apparent power in (1) is used to obtain the instantaneous active and reactive power ($p(t)$, $Q(t)$).

In these conditions, the grid is composed of six components which are the average active and reactive power components (P_0, Q_0) and the four double-frequency components (P_{c2}, P_{s2}, Q_{c2}, Q_{s2}) as [26]

$$p(t) = P_0 + P_{c2}\cos(2\omega t) + P_{s2}\sin(2\omega t) \quad (2)$$

$$q(t) = Q_0 + Q_{c2}\cos(2\omega t) + Q_{s2}\sin(2\omega t) \quad (3)$$

where

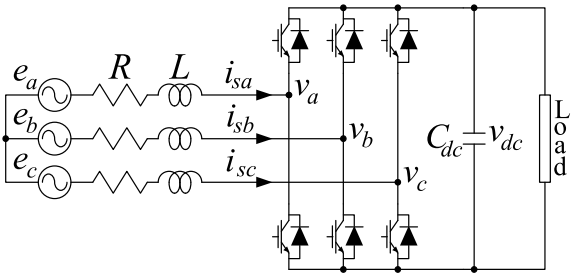

Fig. 1 The voltage source converter circuit

$$P_o = 1.5\left(E_d^p I_d^p + E_q^p I_q^p + E_d^n I_d^n + E_q^n I_q^n\right)$$

$$P_{c2} = 1.5\left(E_d^p I_d^n + E_q^p I_q^n + E_d^n I_d^p + E_q^n I_q^p\right)$$

$$P_{s2} = 1.5\left(E_d^p I_q^p - E_q^p I_d^n - E_d^n I_q^p + E_q^n I_d^p\right)$$

$$Q_o = 1.5\left(-E_d^p I_q^n + E_q^p I_d^p - E_d^n I_q^n + E_q^n I_d^n\right)$$

$$Q_{c2} = 1.5\left(-E_d^p I_q^n + E_q^p I_d^n - E_d^n I_q^p + E_q^n I_d^p\right)$$

$$Q_{s2} = 1.5\left(E_d^p I_d^n + E_q^p I_q^n - E_d^n I_d^p - E_q^n I_q^p\right)$$

E_{dq}^p and E_{dq}^n are the components of the grid d and q-axis voltages, respectively. The unbalanced three-phase grid voltage in dq-axis components are expressed as

$$E_{dq}^p = \left(E_d^p + jE_q^p\right) = \frac{2}{3}\left(E_a^p + aE_b^p + a^2E_c^p\right) \tag{4}$$

$$E_{dq}^n = \left(E_d^n + jE_q^n\right) = \frac{2}{3}\left(E_a^n + aE_b^n + a^2E_c^n\right) \tag{5}$$

where $a = e^{\left(j\frac{2\pi}{3}\right)}$, $E_a^p(t)$ is the positive component of $E_a(t)$, while $E_a^n\ (t)$ is a negative sequential component of $E_a(t)$.

The grid positive and negative currents I_{dq}^p, I_{dq}^n as well as the converter voltage, V_{dq}^p, V_{dq}^n can be defined in the same manner as E_{dq}^p and E_{dq}^n. The conventional electrical equations on the grid side of the VSC are stated as follows:

$$E_{dq}^p = V_{dq}^p + L\frac{d}{dt}I_{dq}^p + j\omega LI_{dq}^p + RI_{dq}^p \tag{6}$$

$$E_{dq}^n = V_{dq}^n + L\frac{d}{dt}I_{dq}^n + j\omega LI_{dq}^n + RI_{dq}^n \tag{7}$$

Using (2)–(7), the reference values for the d and q-axis currents are expressed as:

$$\begin{bmatrix} i_d^{p*} \\ i_q^{p*} \\ i_d^{n*} \\ i_q^{n*} \end{bmatrix} = \frac{2}{3D}V_{dc}^* I_{dc}^* \begin{bmatrix} e_d^p \\ e_q^p \\ -e_d^n \\ -e_q^n \end{bmatrix} \tag{8}$$

where

$$D = (e_d^p)^2 + (e_q^p)^2 - (e_d^n)^2 - (e_q^n)^2 \neq 0$$

where V_{dc}^* is reference DC-link voltage, I_{dc}^* the reference DC-link current reference which can be obtained from the DC-link voltage controller output. When the negative- currents components are adjusted as in (8), the DC-link voltage ripple can be controlled without eliminating the grid-side current unbalance. When the load is sensitive to voltage oscillation, the DC-link ripple illimitation is more important than regulating the grid currents to be balanced. However, to eliminate the unbalance in the grid currents the negative d and q-axis components in (8) should be adjusted to be zero [31–33].

4 Multivariable State Feedback Control

The VSC model in the rotating *dq* reference frame is given by [27]

$$V_d = E_d - R_g I_d - RL_g \frac{dI_d}{dt} + \omega_e L_g I_q \tag{9}$$

$$V_q = E_q - R_g I_q - RL_g \frac{dI_q}{dt} + \omega_e L_g I_d \tag{10}$$

$$P_{grid} = \frac{2}{3}\left(V_d I_d + V_q I_q\right) \tag{11}$$

$$C\frac{dV_{dc}}{dt} = I_{dc} - I_L = \frac{P_{grid}}{V_{dc}} - \frac{P_{Load}}{V_{dc}} \tag{12}$$

where Rg and Lg are the per-phase grid-side resistance and inductance of the coupling inductor, ω_e is grid angular frequency, I_L is the load current, and Co is the DC-link capacitance. P_{grid} and P_{Load} are the active power drawn from the grid and load.

The VSC state-space model for a time-invariant linear multivariable system can be represented in a synchronous frame as [28–30]:

$$\dot{x} = Ax + Bu + Ed \tag{13}$$

$$y = Cx \tag{14}$$

where, the state vector is x, the derivative of the space vector with respect to time is $\dot{x}$, the input or control vector is u, the system matrix is A, the input matrix is B, the disturbance matrix is E, the input disturbance vector is d, the output vector is y, and the output matrix is C.

$$x = \begin{bmatrix} i_{ds} \\ i_{qs} \end{bmatrix},\ u = \begin{bmatrix} v_{dr} \\ v_{qr} \end{bmatrix},\ d = \begin{bmatrix} e_{ds} \\ e_{qs} \end{bmatrix}$$

$$A = \begin{bmatrix} -\frac{R}{L} & \omega \\ -\omega & -\frac{R}{L} \end{bmatrix},\quad B = \begin{bmatrix} -\frac{1}{L} & 0 \\ 0 & -\frac{1}{L} \end{bmatrix}$$

$$E = -B,\ \ C = \begin{bmatrix} 1 & 0 \\ 0 & 1 \end{bmatrix}$$

and ω is grid angular frequency, the source currents are used as the state variables x, while the converter input dq- axis voltages are the input vectors u, the dq-axis grid voltage is the disturbance d, and grid current is the output y.

A. State Feedback Control

When $t \to \infty$, the control target is [38, 39]

$$\dot{x} \to 0 \ \ and\ y \to y_r$$

where y_r is a reference output.

The MSF controller has inaccurate steady-state performance due to model uncertainty and the type of this controller which is considered as a type of proportional control. Therefore, an integral function has to be added to minimize steady-state error. This function is expressed as:

$$p = \int_0^t (y - y_r)dt \tag{15}$$

Assuming that both d and reference y are constant, the derivative of (12) yield to:

$$\dot{p} = y - y_r = Cx - y_r \tag{16}$$

These equations can be written in matrix form and the state model can be expressed as

$$\begin{bmatrix} \dot{x} \\ \dot{p} \end{bmatrix} = \begin{bmatrix} A & 0 \\ C & 0 \end{bmatrix} \begin{bmatrix} x \\ p \end{bmatrix} + \begin{bmatrix} B \\ 0 \end{bmatrix} u + \begin{bmatrix} E & 0 \\ 0 & -I \end{bmatrix} \begin{bmatrix} d \\ y_r \end{bmatrix} \tag{17}$$

In a steady-state, both d and y_r are assumed to be constant which make $\dot{x}$ and error almost zero. Therefore, the state variables, proportional function, and the input vectors in steady-state must follow the following relationship:

$$\begin{bmatrix} E & 0 \\ 0 & -I \end{bmatrix} \begin{bmatrix} d \\ y_r \end{bmatrix} = -\begin{bmatrix} A & 0 \\ C & 0 \end{bmatrix} \begin{bmatrix} x_s \\ p_s \end{bmatrix} - \begin{bmatrix} B \\ 0 \end{bmatrix} u_s \tag{18}$$

where the subscript "s" denotes a steady-state value,
Substituting (15) into (14) yields

$$\begin{bmatrix} \dot{x} \\ \dot{p} \end{bmatrix} = \begin{bmatrix} A & 0 \\ C & 0 \end{bmatrix} \begin{bmatrix} x - x_s \\ p - p_s \end{bmatrix} + \begin{bmatrix} B \\ 0 \end{bmatrix} (u - u_s) \tag{19}$$

To represent the deviations in x_s, p_s, and u_s solutions, a new variable is proposed as:

$$z = \begin{bmatrix} z_1 \\ z_2 \end{bmatrix} = \begin{bmatrix} x - x_s \\ p - p_s \end{bmatrix} \quad (\dot{z} = \begin{bmatrix} \dot{x} \\ \dot{p} \end{bmatrix}) \tag{20}$$

$$v = u - u_s \tag{21}$$

Expressing (17) in the standard state space form as follows:

$$\dot{z} = \hat{A}\, z + \hat{B}\, x \tag{22}$$

where

$$\hat{A} = \begin{bmatrix} A & 0 \\ C & 0 \end{bmatrix}, \; \hat{B} = \begin{bmatrix} B \\ 0 \end{bmatrix}$$

With applying linear state feedback control, the system in (19) is considered to be controllable and it can be written as:

$$\begin{aligned} v &= Kz \\ &= K_1 z_1 + K_2 z_2 \end{aligned} \tag{23}$$

where,
K: feedback gain matrix;
K_1 and K_2: partitioned matrices.
By using Eqs. (16) and (17) the control function in (20) is expressed as

$$u = K_1 x + K_2 p = K_1 x + K_2 \int_0^t (y - y_r) dt \tag{24}$$

B. Feedforward Control

It is expected to have zero static errors by applying the integral controller. This could be true in small disturbances, however, in large transients and disturbances the dynamic errors may be large. The dynamic performance can be improved during the large disturbances by adding a feedforward controller. The disturbance and reference inputs are both used to extract the feedforward control equations and the control system is defined as follows:

$$\begin{bmatrix} \dot{x} \\ \tilde{y} \end{bmatrix} = \begin{bmatrix} A & B \\ C & 0 \end{bmatrix} \begin{bmatrix} x \\ u \end{bmatrix} + \begin{bmatrix} E & 0 \\ 0 & -I \end{bmatrix} \begin{bmatrix} d \\ y_r \end{bmatrix} \tag{25}$$

where $\tilde{y} = y - y_r$,

The steady-state condition is reached when the left-hand side of (22) when the steady-state inputs and variable state are as follows:

$$\begin{bmatrix} x_s \\ u_s \end{bmatrix} = -\hat{G}^{-1} \hat{H} \begin{bmatrix} d \\ y \end{bmatrix} \tag{26}$$

where

$$\hat{G} = \begin{bmatrix} A & B \\ C & 0 \end{bmatrix}, \ \hat{H} = \begin{bmatrix} E & 0 \\ 0 & -1 \end{bmatrix}$$

The variables deviations from the steady-state give new variables which are expressed as:

$$\tilde{x} = x - x_s \quad (\dot{\tilde{x}} = \dot{x}), \tilde{u} = u - u_s \tag{27}$$

By substituting (24) into (24) the steady-state deviations are given by,

$$\dot{\tilde{x}} = A\,\tilde{x} + B\,\tilde{u}, \quad \tilde{y} = C\,\tilde{x} \tag{28}$$

By substituting (25) and (24) into (21), we get

$$u = K_1 x + [-K_1 \quad I] \begin{bmatrix} x_s \\ u_s \end{bmatrix} \tag{29}$$

Equation (22) is then used to define the feedforward by substituting into (26) as follows:

$$u = K_1 x + K_{ff} \begin{bmatrix} d \\ y_r \end{bmatrix} \tag{30}$$

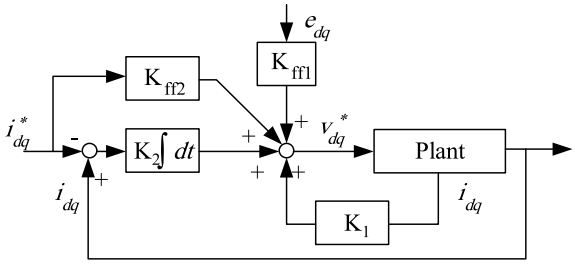

Fig. 2 Block diagram for MSF control

where k_{ff} is the feedforward gain and is defined as

$$K_{ff} = [K_1 \quad -I]\hat{G}^{-1}\hat{H}$$
$$= [K_{ff1} \quad K_{ff2}]$$

The control equation is then determined by substituting the integral controller (12) into (27) to be comprised from the state variables, reference inputs, and disturbance as follows:

$$u = K_1 x + K_2 \int_0^t (y - y_r)dt + K_{ff} \begin{bmatrix} d \\ y_r \end{bmatrix} \tag{31}$$

Figure 2 shows the MSF control block diagram including the feedback and feedforward components. The detailed proposed control system is shown in Fig. 3 where the DC voltage V_{dc} is controlled to minimize the DC-link ripples which affect the connected load. A PI controller is used to control the DC voltage, while the current controllers for the positive and negative are MSF controllers as shown in the figure. The output reference DC-link current I^*_{dc} is used to calculate the converter reference power P^*. By using the measured and calculated voltages, currents, and power, Eq. (8) is then used to extract the current controller reference dq-axis currents. The state feedback matrix is then determined from the dq-axis currents and grid voltages to get the voltage reference which is then used as input to the modulator.

5 Experimental Results

Experiments are conducted to verify the validity of the proposed algorithm. The switching frequency of the IGBT PWM converter is 5 [kHz], and the sampling periods of voltage control and current control are 100usec. The three-phase input voltage is 100Vrms, the DC output voltage command is 150 [V], and the converter load is 50 [Ω].

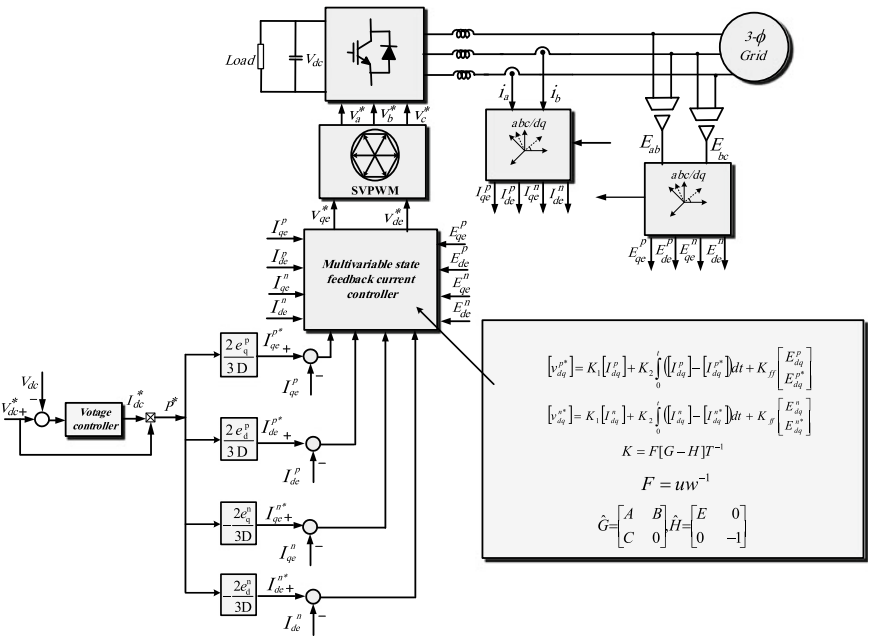

Fig. 3 Overall control block diagram of PWM converter

Figure 4 shows the waveform of the distorted and unbalanced grid voltage. Figure 5 shows the waveforms of a typical current controller under the conditions of Fig. 10. The input current in Fig. 5a contains harmonics and Fig. 5b shows that the DC-link voltage pulsates at twice the frequency of the power supply.

Next, Fig. 6 shows the waveform of adding both harmonic current controller and reverse-phase current controller. Figure 6a does not include harmonic currents, and Fig. 6b shows the waveforms when the DC-link voltage ripple adds almost all current controllers.

If the ripple of DC voltage due to unbalance does not greatly affect the control of the load or inverter connected to the DC terminal, it is recommended to set the reverse-phase current command to 0 to eliminate the unbalance of input current. Figure 7 shows the result of this control. Figure 7a shows that the input current is

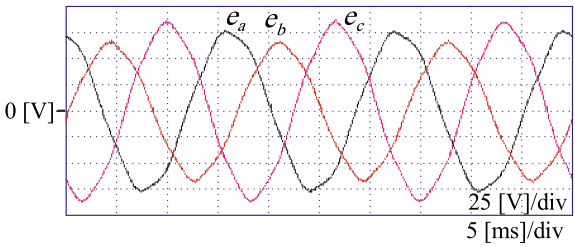

Fig. 4 Unbalanced grid voltage

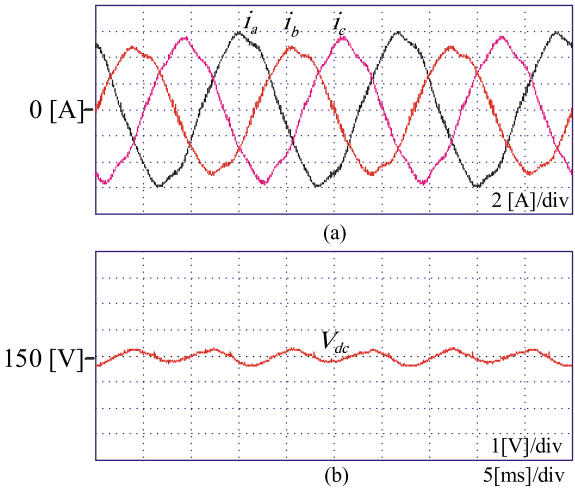

Fig. 5 Conventional current control at nonideal source voltage **a** three-phase input current **b** DC-link voltage

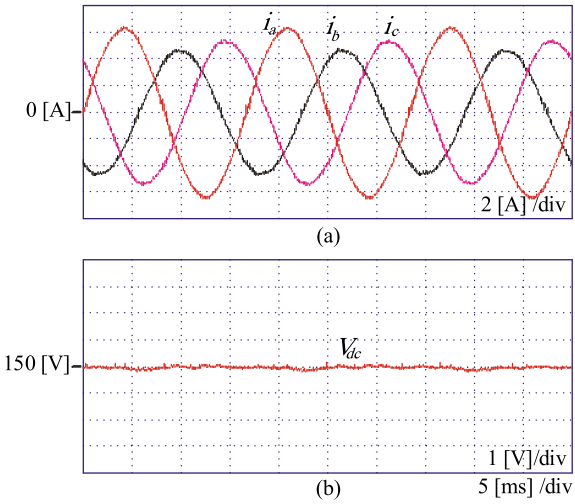

Fig. 6 Elimination of DC-link voltage ripples **a** three-phase input current **b** DC-link voltage

balanced, and Fig. 7b shows a slight increase in the ripple of the DC-link voltage in this case.

6 Conclusion

In this chapter, a control strategy for a three-phase PWM converter in case of unbalanced grid voltage has been proposed. The controller of the converter generally consists of a voltage controller in the outer loop and a current controller in the inner

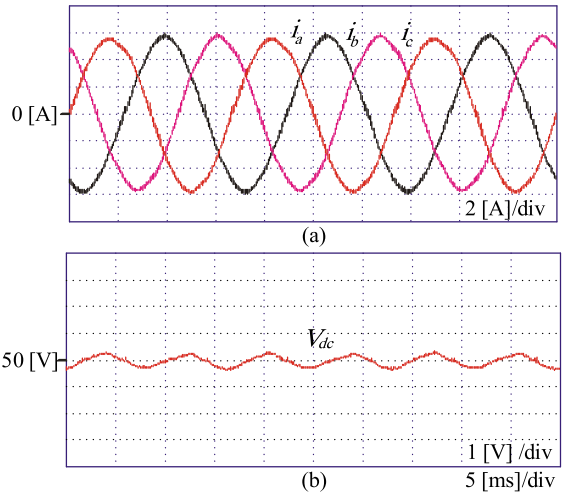

Fig. 7 Grid current balancing control without DC-link voltage
a three-phase input current
b DC-link voltage

loop. The current controller in this study consists of four independent control loops: positive and negative- current controllers to maintain the input current balance and to eliminate the ripple of the DC terminal voltage appearing. The proposed controller exhibited excellent performance in minimizing the DC-link voltage ripple and in eliminating the unbalance of grid-side current.

References

1. Abo-Khalil AG, Kim HG, Lee DC, Seok JK (2004) Maximum output power control of wind generation system considering loss minimization of machines. Proc IECON'04, pp 1676–1681
2. Khaled U, Eltamaly AM, Beroual A (2017) Optimal power flow using particle swarm optimization of renewable hybrid distributed generation. Energies 10(7):1013
3. Qin H, Kimball JW (2014) Closed-loop control of DC-DC dual-active-bridge converters driving single-phase inverters. Power Electron IEEE Trans 29(2):1006–1017
4. Lin JL, Yao WK, Yang SP (2006) Analysis and design for a novel single-stage high power factor correction diagonal half-bridge forward AC-DC converter. Circ Syst IEEE Trans 53(10):2274–2286
5. Tsang KM, Chan WL (2005) Adaptive control of power factor correction converter using nonlinear system identification. Power Appl IEEE Proc Electr 152(3):626–633
6. Pena RS, Cardenas RJ, Clare JC, Asher GM (2001) Control strategies for voltage control of a boost type PWM converter. IEEE 32nd Power Elec. Spec. Conf, PESC'01, vol 2, pp. 730–735
7. Chang E-C, Liang T-J, Chen J-F, Chang F-J (2008) Real-time implementation of grey fuzzy terminal sliding mode control for PWM DC-AC converters. . IET Power Electron 1:235–244
8. Cecati C, Dell'Aquila A, Lecci A, Liserre M (2005) Implementation issues of a fuzzy logic-based three-phase active rectifier employing only voltage sensors. IEEE Trans Ind Electron 52:378–385
9. Allag A, Hammoudi M, Mimoune SM, Ayad MY, Becherif M, Miraoui A (2007) Tracking control via adaptive backstepping approach for a three phase PWM AC-DC converter. IEEE international symposium on industrial electronics, ISIE'07, pp 371–376

10. Escobar G, Chevreau D, Ortega R, Mendes E (2001) An adaptive passivity-based controller for a unity power factor rectifier. IEEE Trans Control Syst Technol 9:637–644
11. Harnefors L, Zhang L, Bongiorno M (2008) Frequency-domain passivity-based current controller design. IET Power Electron 1:455–465
12. Shtessel Y, Baev S, Biglari H (2008) Unity power factor control in three-phase AC/DC boost converter using sliding modes. IEEE Trans Ind Electron 55:3874–3882
13. Eltamaly AM, Alolah AI, Abdel-Rahman MH (2010) Modified DFIG control strategy for wind energy applications. In: SPEEDAM 2010. IEEE, pp 653–658
14. Mendalek N, Al-Haddad K, Fnaiech F, Dessaint LA (2003) Nonlinear control technique to enhance dynamic performance of a shunt active power _lter. IEE Proc Electric Power Appl 150:373–379
15. Lee T-S (2003) Input-output linearization and zero-dynamics control of three-phase AC/DC voltage-source converters. IEEE Trans Power Electron 18:11–22
16. Burgos RP, Wiechmann EP (2005) Extended voltage swell ride-through capability for PWM voltage-source rectifiers. IEEE Trans Ind Electron 52:1086–1098
17. Lee T-S, Tzeng K-S (2002) Input-output linearizing control with load estimator for three-phase AC/DC voltage-source converters. In: IEEE 33rd Power Electr. Spec. Conf., PESC'02, vol. 2, pp 791–795
18. Nikkhajoei H, Iravani R (2007) Dynamic model and control of AC/DC/AC voltage-sourced converter system for distributed resources. IEEE Trans Power Del 22:1169–1178
19. Savaghebi M, Jalilian A, Vasquez JC (2012) A secondary control level to focus the grid voltage and does not concern the local control objectives of the VSC. IEEE Trans Smart Grid 3(2):797–807
20. Eltamaly AM, Khan AA (2011) Investigation of DC link capacitor failures in DFIG based wind energy conversion system. Trends Electr Eng 1(1):12–21
21. Teodorescu R, Blaabjerg FM, Liserre M (2006) Proportional resonant controllers and filters for grid-connected voltage-source converters. IEE Proc-Electr Power Appl 153:750–762
22. Lascu C, Asiminoaei L, Boldea I, Blaabjerg FM (2007) High performance current controller for selective harmonic compensation in active power filters. IEEE Trans Power Electron 22:1826–1835
23. Dawei Z, Lie X, Williams BW (2010) Model-based predictive direct power control of doubly fed induction generators. IEEE Trans Power Electron 25:341–351
24. Cort'es P, Rodriguez J, Antoniewicz P, Kazmierkowski M (2008) Direct power control of an AFE using predictive control. IEEE Trans Power Electron 23:2516–2553
25. Ab-Khalil AG (2015) Control system of DFIG for Wind Power Generation Systems. LAP LAMBERT Academic Publishing, ISBN-10: 3659649813, ISBN-13: 978–3659649813
26. Abo-Khalil AG, Abdulbasser M (2016) Multivariable state feedback control of three-phase voltage source-PWM current regulator. Middle-East J Sci Res 24(3):10
27. Abo-Khalil AG, Ab-Zied H (2012) Sensorless control for DFIG wind turbines based on support vector regression. Industrial electronics conference IECON, Canada
28. Abokhalil AG (2019) Grid connection control of DFIG for variable speed wind turbines under turbulent conditions. Int J Renew Energy Res (IJRER) 9(3):1260–1271
29. Abo-Khalil AG, Alghamdi A, Tlili I, Eltamaly A (2019) A current controller design for DFIG-based wind turbines using state feedback control. IET Renew Power Generation 13(11):1938–1949
30. Abo-Khalil AG, Alghamdi AS, Eltamaly AM, Al-Saud MS, Praveen PR, Sayed K (2019) Design of state feedback current controller for fast synchronization of DFIG in wind power generation systems. Energies 12(12):2427

31. Abo-Elyousr FK, Youssef A (2018) Optimal PI microcontroller-based realization for technical trends of single-stage single-phase grid-tied PV. Eng Sci Technol Int J 21:945–956
32. Abdelwahab SAM, Yousef AM, Ebeed M, Abo-Elyousr FK, Elnozahy A, Mohammed M (2020) Optimization of PID controller for hybrid renewable energy system using adaptive sine cosine algorithm. Int J Renew Energy Res 10(2):669–677
33. Eltamaly AM, Alolah AI, Abdel-Rahman MH (2011) Improved simulation strategy for DFIG in wind energy applications. Int Rev Model Simul 4(2)